Molecular fluorescence significantly enhanced by gold nanoparticles@zeolitic imidazolate framework-8

Yuyi Zhang(张钰伊)[1], Yajie Bian(卞亚杰)[1], Wei Zhang(张炜)[1], Yiting Liu(刘易婷)[1], Xiaolei Zhang(张晓磊)[1,2,†], Mengdi Chen(陈梦迪)[1,‡], Bingwen Hu(胡炳文)[1], and Qingyuan Jin(金庆原)[1,3,§]

[1] *State Key Laboratory of Precision Spectroscopy, Shanghai Key Laboratory of Magnetic Resonance, School of Physics and Electronic Science, East China Normal University, Shanghai* 200241, *China*

[2] *Collaborative Innovation Center of Extreme Optics, Shanxi University, Taiyuan* 030006, *China*

[3] *Department of Optical Science and Engineering, Fudan University, Shanghai* 200433, *China*

(Received 28 May 2022; revised manuscript received 14 July 2022; accepted manuscript online 18 July 2022)

Noble metal nanoparticles exhibit unique surface plasmon resonance dependent optical properties. On this basis, gold nanoparticles (AuNPs) encapsulated in metal–organic frameworks (MOFs) can form AuNPs@MOFs composites to modulate the optical properties of fluorescent molecules, which is less reported. In this paper, based on the fluorescence enhancement effect of AuNPs on 2-(2-hydroxyphenyl)-1H-benzimidazole (HPBI) molecules, zeolitic imidazolate framework-8 (ZIF-8) crystals with structural stability were introduced. AuNPs@ZIF-8 exhibited a significantly pronounced fluorescence enhancement of the HPBI molecules. In addition, by comparing the fluorescence characteristics of the HPBI molecules adsorbed on AuNPs@ZIF-8 and those captured in AuNPs@ZIF-8, we found that the ZIF-8 can act as a spacer layer with highly effective near-field enhancement. All our preliminary results shed light on future research on the composite structures of noble metal particles and MOFs for fluorescent probes and sensing applications.

Keywords: ZIF-8, gold nanoparticles, fluorescence spectra, fluorescence lifetime

PACS: 42.70.–a **DOI:** 10.1088/1674-1056/ac81aa

1. Introduction

Metal–organic frameworks (MOFs) are a type of microporous material made up of assembling metal ions and organic ligands. MOFs have a large specific surface area, uniform but adjustable cavities, and tunable chemical characteristics. These properties make them ideal for a wide range of applications, including gas storage,[1,2] chemical separation,[3] catalysis,[4,5] sensing,[6] and drug delivery.[7] By serving as unique host matrices for a variety of functional species, MOFs have the potential to serve as the foundation for novel composite materials that exhibit new catalytic, optical and electrically conductive[8–10] behaviors when compared with pure MOF counterparts.[11]

MOFs can be utilized to stabilize size-tunable metal nanoparticles because of their large surface area and well-defined pore structure. Due to the high porosity properties of MOFs, it is possible to simultaneously perform the original functions of the encapsulated metal nanoparticles. This makes "metal nanoparticles@MOFs" systems particularly interesting for heterogeneous catalysis, gas storage and chemical sensing.[12] Multi-shelled hollow MOF microcrystals are excellent composites for hosting multiple guests, while performing controlled communication such as energy transfer (ET). Tsung *et al.* introduced rhodamine 6G (R6G) and 7-amino-4-(trifluoromethyl) coumarin as its molecular guests, and palladium nanoparticles as heterogeneous guests into the multi-shelled hollow zeolitic imidazolate framework-8 (ZIF-8).[13] These composites combine adjustable properties at the molecular level with encapsulation capabilities. Chen *et al.* found that ZIF-8 coated gold nanorods (AuNRs) could be employed for improved photothermal therapy and stability.[14] This suggests that AuNRs@ZIF-8 strongly convert near-infrared irradiation into thermal energy.

Despite studies concerning metal nanoparticles@MOFs, very few reports have focused on the fluorescent properties of the composite structures of noble metal particles and MOFs. Metal-enhanced fluorescence occurs mainly as a result of the interaction between the excited state and the near field of the excited metal nanoparticles. Due to the rapid decay of near fields around the metal nanoparticles, the distance between the fluorophores and the metallic nanoparticles might impact the surface-enhanced fluorescence process drastically.[15] Studies have previously focused on surface-enhanced Raman scattering (SERS) of metal nanoparticles@MOFs. Researchers reported a simple and versatile approach to synthesizing metal@ZIF-8 hybrid structures, and gained a better understanding of the molecular sieving effect and the plasmonic properties of the encapsulated metal nanoparticles, i.e., the size selection for molecular diffusion through ZIF-8, using SERS spectra.[16] Hupp and Van Duyne *et al.* used MOF films

†Corresponding author. E-mail: xlzhang@admin.ecnu.edu.cn
‡Corresponding author. E-mail: mdchen@lps.ecnu.edu.cn
§Corresponding author. E-mail: qyjin@fudan.edu.cn

© 2023 Chinese Physical Society and IOP Publishing Ltd

to make functional modifications to surface Raman-active structures, called silver "films-over-nanospheres" (FONs). Most of the vapors (like benzene, toluene, pyridine, nitrobenzene, and 2,6-ditertbutylpyridine) cannot be adsorbed on metal surfaces that have not been functionally modified, so the MOF films play a key role in confining molecules to nanoscale hotspots of the FONs and also represent a novel approach to vapor-phase SERS sensing.[17]

Researchers were drawn to ZIF-8 because of its chemical robustness and thermal stability. Its structure is sodalite zeolite-like, with large cavities (11.6 Å) and small apertures (3.4 Å).[18] Aside from its structural advantages, the researchers discovered that the luminescence intensity of ZIF-8 is very sensitive to Cu^{2+} and Cd^{2+} ions as well as tiny molecules like acetone.[19] Chen *et al.* also showed that ZIF-8 can be used as effective scaffolding materials to encapsulate pyrene molecules, which can be used to detect the oxygen within ZIF-8 pores.[20] Therefore, encapsulating metal nanoparticles into ZIF-8 and investigating their ability to modulate the fluorescence of molecules seems appealing, but as yet there is not much in-depth research.

In this paper, we focus on molecular fluorescence modulated by gold nanoparticles@ZIF-8 composites. The composites were made by combining crystallized ZIF-8 with encapsulated gold nanoparticles (AuNPs) modified with polyvinylpyrrolidone in methanol at room temperature (PVP). Pre-synthesized gold nanoparticles were enclosed in the developing ZIF-8 crystals using this strategy.[11] Herein we prepared AuNPs@ZIF-8 and compared its enhanced fluorescence ability for 2-(2-hydroxyphenyl)-1H-benzimidazole (HPBI) with AuNPs and ZIF-8. Furthermore, the role of ZIF-8 was investigated by comparing the fluorescence characteristics of the HPBI molecules adsorbed on AuNPs@ZIF-8 and those captured in AuNPs@ZIF-8. Our work offers a potential exploration of AuNPs@ZIF-8 in fluorescent probe applications.

2. Method

2.1. Materials characterization

Scanning electron microscopy (SEM, Zeiss Gemini 450) and transmission electron microscopy (TEM, JEM-2100F) were used to analyze the structures and morphologies. All of the luminescence emission spectra were acquired using an optical fibre and a liquid nitrogen cooled charge coupled device spectrometer (Princeton Instruments). An optical fibre coupled to a microchannel plate photomultiplier tube (Hamamatsu) was used to achieve the fluorescence lifetime, which was paired with a time-correlated single photon counting technique (TCSPC, Edinburgh Instruments). The samples were excited using a 375 nm pulse picosecond semiconductor laser (Advance Laser System). The absorption spectrum was measured using a Shimadzu UV/vis spectrophotometer. A scanning tunnelling microscope (STM, CREATEC) was used to examine the distribution and size of HPBI and R6G molecules on the substrate.

2.2. Synthesis of AuNPs and AuNPs@ZIF-8

AuNPs were prepared with a sodium citrate reduction method of $HAuCl_4$.[21] The gold colloidal solution stabilized with PVP was rinsed with deionized water before being centrifuged and dispersed in 20 mL of methanol (8000 rpm, 10 min). PVP is an amphiphilic, non-ionic polymer that has been used as a surfactant to stabilize gold nanoparticles in methanol[22] and as a capping agent to help control the size and shape of nanoparticles during their synthesis.[23]

PVP was used to functionalize the surfaces of the gold nanoparticles, which were manufactured using conventional techniques.[21] The approach was originally shown for AuNPs with a diameter of 120 nm. Hmim (100 mM, 5 mL) and 1-MI (50 mM) methanolic solutions were combined quickly with $N_2O_6Zn6H_2O$ (25 mM, 5 mL) methanolic solutions, and the combination was kept at room temperature for 24 h without stirring. The produced particles were collected using centrifugation and then washed in methanol several times before being redispersed in methanol. Based on the number of AuNPs added, for the sample named AuNPs@ZIF-8-2 there were 10 additional AuNPs to AuNPs@ZIF-8-1. More synthesis details of ZIF-8, HPBI@ZIF-8 and HPBI on ZIF-8 are listed in the supporting information.

3. Results and discussion

Surface plasmon resonance (SPR), which refers to the coherent oscillation of free electrons on the gold surface, determines the optical properties of AuNPs. Waves propagating along a planar metal surface produce surface plasmon polaritons, and localized surface plasmon resonance (LSPR) occurs when the surface plasmon is restricted to metal nanoparticles with dimensions smaller than the wavelength of the excitation.[17,24,25] The interaction between the excited state of the emitter and the near field of the excited metal nanoparticles causes metal-enhanced fluorescence. As a result of the rapid decrease in the near field around metal nanoparticles, the distance between the fluorophore and the metal nanoparticle can have a significant impact on the process of surface-enhanced fluorescence.[26–28] When the fluorophore is in close proximity to the metal nanoparticles (direct contact or a distance of only a few nanometers), the advantage of LSPR excitation will be eliminated by the predominance of non-radiative relaxation rate, leading to fluorescence quenching.[29–31]

These AuNPs have a morphology of around 120 nm (Fig. 1(a)). The AuNPs showed a broad strong absorption peak located at around 560 nm originating from the SPR

(Fig. 1(b)).[19,32] Based on the above analysis, we considered the direct mixing of AuNPs with HPBI molecules to observe the effect of AuNPs on the molecular fluorescence properties. There were no changes in photoluminescence (PL) emission when we added AuNPs into HPBI solution, but after 24 h, the emission peak was about 1.8-fold enhanced compared to pure HPBI, and the emission peak was about 14 nm red-shifted. At this time the AuNP surface was wrapped with PVP, and even when the molecules are directly mixed with gold nanoparticles, there is no fluorescence quenching. Due to the LSPR of the AuNPs, there is a certain enhancement effect of HPBI fluorescence (Fig. 1(c)). In principle, the plasmon resonance affects both the radiative rate enhancement and the scattering efficiency of the nanoparticle. As a result, any mechanism that changes the plasmon resonance of nanoparticles, both externally and internally, has an impact on the enhancement of nearby fluorophores.[33]

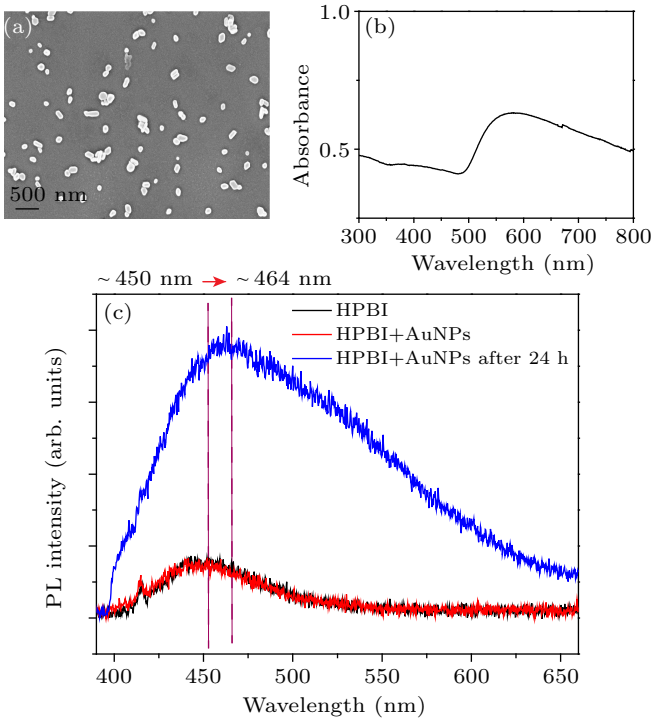


Fig. 1. (a) SEM images of AuNPs: ~ 120 nm. (b) UV/vis absorption spectra of AuNPs. (c) Fluorescence emission spectra of HPBI and HPBI + AuNPs.

We found that with the LSPR properties of AuNPs, free AuNPs in solution have a particular fluorescence enhancement effect on HPBI molecules, but we expected that the fluorescence modulation ability of AuNPs may play a more pronounced role. We consider using the framework structure of ZIF-8 crystals to wrap the AuNPs, on one hand, ZIF-8 restricts the movement of AuNPs in solution, while on the other hand, the pore size of ZIF-8 can play a role in restricting the molecules in the pore size of HPBI molecules smaller than the pore size of ZIF-8.

Nanoparticles/MOFs composites can be prepared by either using MOFs as a template to allow nanoparticles to enter the cavities through the pores[12,34–37] or by wrapping presynthesized nanoparticles into the MOFs.[38,39] In this paper, AuNPs@ZIF-8 were obtained mainly by growing ZIF-8 crystals around PVP modified AuNPs. The dual-ligand ZIF-8 precursor containing both Hmim and 1-MI was adopted to encapsulate the PVP functionalized AuNPs. In order to control the distribution of AuNPs in the ZIF-8 crystals, we added 5 mM 1-MI to aggregate the AuNPs in the ZIF-8 crystals. Corresponding to the concentration of AuNPs we added, we received two different AuNPs@ZIF-8. For the more AuNPs@ZIF-8, the number of AuNPs added is 10 times as few AuNPs@ZIF-8, and we define the few AuNPs@ZIF-8 as AuNPs@ZIF-8-1 and the more AuNPs@ZIF-8 as AuNPs@ZIF-8-2. SEM and TEM images of AuNPs@ZIF-8-1 and AuNPs@ZIF-8-2 are shown in Figs. 2(a)–2(d). The ZIF-8 crystals were synthesized through rapid mixing of a solution of zinc acetate with a solution of Hmim and 1-MI at room temperature. As shown in Fig. 2(e), the crystal size of ZIF-8 was found to be around 1300 nm by SEM.

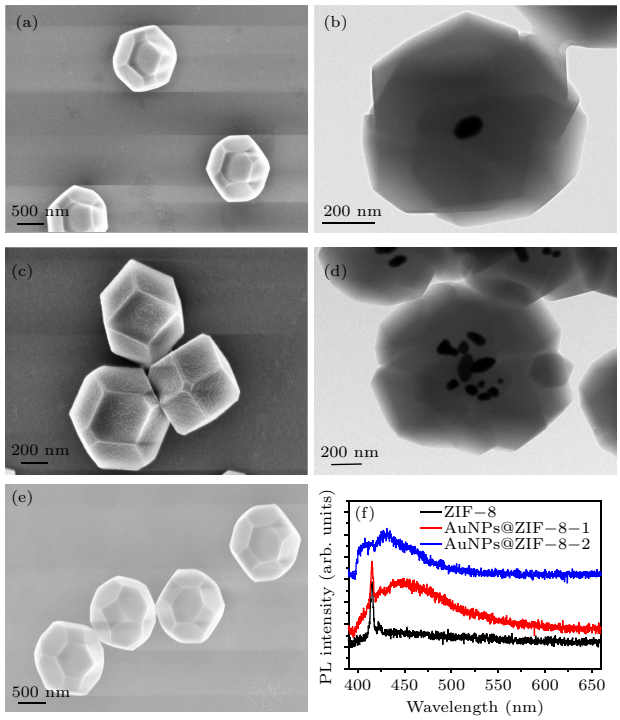


Fig. 2. (a) SEM image of AuNPs@ZIF-8-1. (b) TEM image of AuNPs@ZIF-8-1. (c) SEM image of AuNPs@ZIF-8-2. (d) TEM image of AuNPs@ZIF-8-2. (e) SEM image of ZIF-8. (f) Fluorescence spectra of ZIF-8, AuNPs@ZIF8-1, AuNPs@ZIF8-2.

Figure 2(f) shows the emission spectrum of the pristine crystals of ZIF-8 and AuNPs@ZIF-8. The emission peak of ZIF-8 was located at 450 nm near the emission peak of AuNPs@ZIF-8-1, but the intensity was much lower than AuNPs@ZIF-8-1. For AuNPs@ZIF-8-2, the emission peak is located at 430 nm with multi-peaks. It has been reported that MOFs with transition-metal ions without unpaired electrons can produce luminescent materials based on organic

linkage bonds. The fluorescence emission peak of ZIF-8 overlaps with the emission peak position of the free ligand 2-methylimidazole and is red-shifted relative to the free ligand (the emission of Hmim shifts from 425 nm to 450 nm for ZIF-8), from which it is judged that ZIF-8 fluorescence emission originates from the coordination effect of Hmim with Zn^{2+}.[19] When we enveloped a small number of AuNPs into ZIF-8, the emission peak shift in the spectrum showed that the few AuNPs had no obvious effect on the energy conversion. During the synthesis of AuNPs@ZIF-8-2, we injected 10 times more AuNPs compared to AuNPs@ZIF-8-1, and the other sample amounts were not changed, which resulted in partial crystal agglomeration, and at this time the sample size was not homogeneous with the overall occurrence of multiple peaks.

The role that ZIF-8 played in tuning HPBI molecular fluorescence has already been studied in our previous work,[40] and in the present work the fluorescence results of ZIF-8 mixed with HPBI molecules were mainly used as a comparison with AuNPs@ZIF-8. In our previous work,[40] we had already investigated that when ZIF-8 was added to the HPBI solution, the PL intensity of the mixture increased as the blending time increased from 5 min to 120 min. From 120 min to 240 min, the increment slowed down, and by the end of 16 h, the PL intensity had no obvious enhancement. Based on the results, the blending time was chosen to be 24 h in the current work. We began by investigating the emission properties of HPBI and HPBI + ZIF-8 at room temperature. HPBI powder was deposited on the surface of the Au(111) substrate by thermal evaporation under an ultrahigh vacuum environment, and the STM topograph at ~ 80 K is shown in Fig. 3(a). The size of the HPBI is roughly 3×7 Å based on the STM figure and HPBI chemical structure.

Figure 3(b) shows fluorescent spectra of HPBI at various concentrations (0.01 mM, 0.05 mM, 0.1 mM, 0.125 mM, 0.15 mM, 0.2 mM, and 0.25 mM), with characteristic peaks at 455 nm. HPBI and its derivatives are an important class of fluorescent compounds that have attracted interest due to their excited-state intramolecular proton transfer (ESIPT).[41–43] When 100 μL ZIF-8 was added to 1 mL HPBI solution, a significant increase in the fluorescence intensity of the mixture was observed and the fluorescence emission peak position blue-shifted from 450 nm to 410 nm (Fig. 3(c)). With the change in concentration of HPBI solution mixed with ZIF-8, the fluorescence intensity of the mixture varied nonlinearly. The integrated signal intensity was plotted as a function of HPBI concentration in Fig. 3(d). We defined $\Delta I = I_{(\mathrm{ZIF-8+HPBI})}/I_{\mathrm{HPBI}}$ and used a curve to calculate the variation in fluorescence intensity ratio at different concentrations. The fluorescence intensity of the mixture was significantly enhanced when the concentration ranged from 0.01 mM to 0.1 mM, and ΔI reached its maximum at HPBI concentrations corresponding to 0.1 mM, which is about a 47.6-fold enhancement. Continuing to increase the concentration of HPBI, it was found that ΔI began to decrease. When the concentration continued to increase to 0.15 mM, ΔI decreased to 6.0, which indicated that the fluorescence enhancement effect of ZIF-8 on HPBI was significantly weakened. From these results, we determined that the fluorescence intensity is enhanced with the aggregation of HPBI molecules, and that the aggregation capacity is limited, reaching saturation at a molecular concentration of 0.1 mM. The saturation concentration is equal to what we previously received.[40] As the solution concentration continues to increase, it can be found that the concentration has almost no effect on ΔI and remains at a lower enhancement intensity ratio. The mixture was also accompanied by a blue shift, which can be attributed to Zn^{2+}.[40] All results indicate that the pores of ZIF-8 can limit the vibration and rotation of the molecules, resulting in increased emission efficiency,[44] and that there is a π–π stacking between the benzene ring of HPBI and the imidazole ring in the ZIF-8 structure.[45,46]

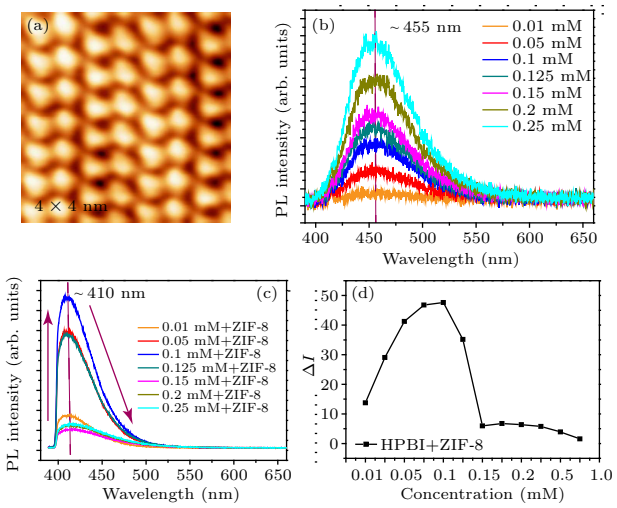


Fig. 3. (a) HPBI on Au(111) in a typical STM image (4 nm × 4 nm, −2.7 V, 10 pA). (b) Fluorescence spectra of HPBI at various concentrations under excitation at 375 nm. (c) Fluorescence spectra of HPBI following the addition of ZIF-8 at various concentrations. (d) ΔI denotes the increased fluorescence intensity of HPBI with various concentrations after adding ZIF-8.

We have already obtained the effects of ZIF-8 crystals and AuNPs on the fluorescence properties of HPBI molecules. Coupled with the fact that the ZIF-8 crystal itself already has a significant fluorescence enhancement effect on the HPBI molecule, we expect to further investigate the fluorescence modulation effect of the AuNPs@ZIF-8 composite on the molecules. We introduced AuNPs into ZIF-8 to obtain AuNPs@ZIF-8 composites, to further investigate the role of the LSPR effect of AuNPs in the modulation of molecular fluorescence intensity. We chose 0.1 mM HPBI mixed with AuNPs@ZIF-8-1 and AuNPs@ZIF-8-2, separately, and the

fluorescence intensity of the mixture was also significantly enhanced and the peak shape was similar to that of HPBI + ZIF-8 (Fig. 4(a)). The emission spectroscopy was tested at 12 h and 24 h after mixing, and ΔI was obtained by comparing the mixture to a sample of HPBI fluorescent intensity. The concentrations corresponding to the maximum values of the fluorescence enhancement intensity ratios were all at 0.1 mM. It was found that the results of HPBI + AuNPs@ZIF-8-1 were similar to those of HPBI + ZIF-8 (Figs. 4(b) and 4(d)), but ΔI of HPBI + AuNPs@ZIF-8-2 was significantly enhanced from 40.1 to 74.8 during 12 h (Fig. 4(c)), for which the enhancement was even more pronounced than HPBI + ZIF-8 and HPBI + AuNPs@ZIF-8-1. This may be due to the framework structure of ZIF-8, which formed a spacer layer wrapped around AuNPs, and in turn improved the fluorescence emission efficiency of HPBI + AuNPs@ZIF-8-2 with the plasmon resonance of AuNPs. The fluorescence intensity increased significantly with time, further indicating that the pore size of ZIF-8 provided a channel for the aggregation of HPBI.[21]

Using the TCSPC approach, we measured the emission lifetimes of HPBI, ZIF-8, and HPBI + ZIF-8 to corroborate the aforementioned phenomena. The curve of HPBI + ZIF-8 (purple) was located between the ZIF-8 lifetime (red) and the lifetime of HPBI (black). The presence of Zn^{2+} in ZIF-8 hindered the ESIPT process in HPBI. Furthermore, the fluorescence lifetime of the HPBI + ZIF-8 mixture was shorter than that of a pure HPBI molecule and was accompanied by fluorescence emission from the π–π^* transition due to the pore size of ZIF-8 limiting the rotation of the HPBI molecule. When the fluorescence lifetimes of ZIF-8 and AuNPs@ZIF-8 are compared, they are nearly identical, indicating that the presence or absence of gold particle wrapping has no effect on energy transmission; the fluorescence lifetimes of HPBI + ZIF-8, HPBI + AuNPs@ZIF-8-1, and HPBI + AuNPs@ZIF-8-2 were the same and were placed between HPBI and ZIF-8/AuNPs@ZIF-8 (Fig. 5).

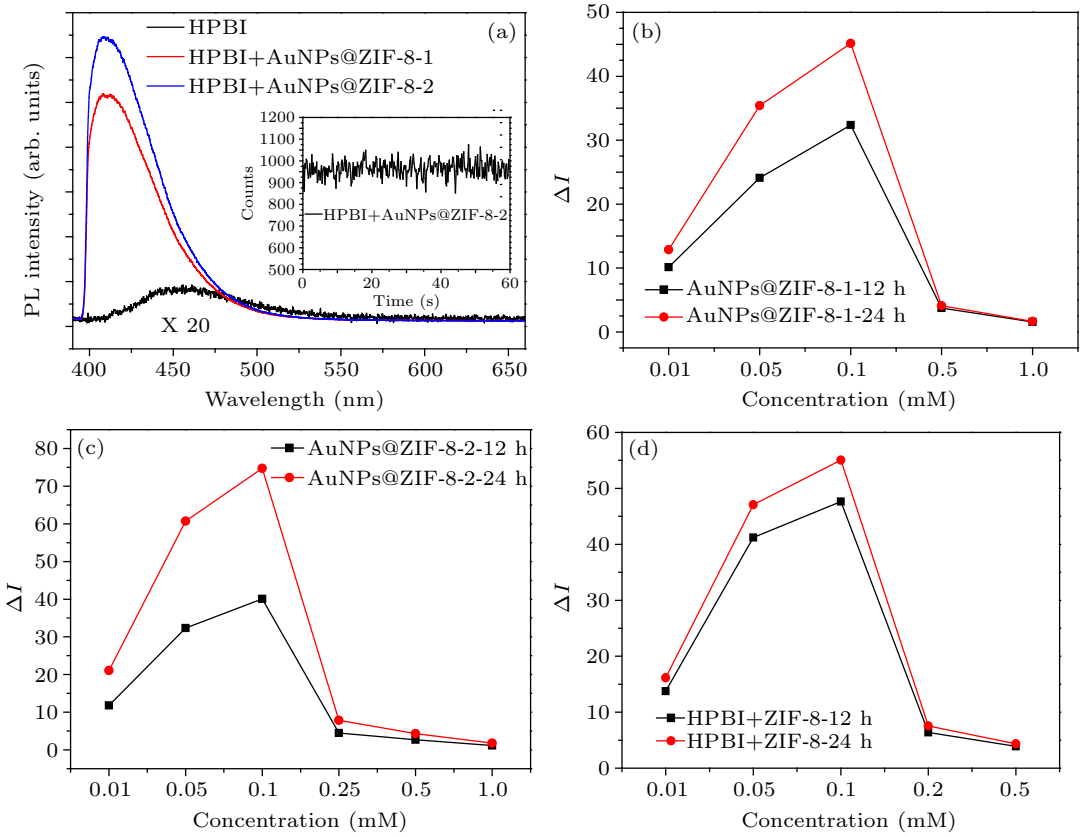


Fig. 4. (a) Fluorescence spectra of HPBI + AuNPs@ZIF-8-1 and HPBI + AuNPs@ZIF-8-2 (insert: the change of photon counts during 1 min). (b) Comparison of ΔI denotes the increased fluorescence intensity of HPBI at various concentrations after adding AuNPs@ZIF-8-1 at 12 h and 24 h. (c) Comparison of ΔI denotes the increased fluorescence intensity of HPBI at various concentrations after adding AuNPs@ZIF-8-2 at 12 h and 24 h. (d) Comparison of ΔI denotes the increased fluorescence intensity of HPBI at various concentrations after adding ZIF-8 at 12 h and 24 h.

Detailed lifetimes are listed in Table 1. Emission lifetimes (τ) were calculated by fitting the decays to the following function: $I(t) = A_1 e^{-t/\tau_1} + A_2 e^{-t/\tau_2}$, where A is the pre-exponential factor and t is time.[47] The longer lifetime decay component increases at the lower emission energy levels and is accompanied by a delay in fluorescence emission, a result that illustrates the interaction between individual molecules in HPBI during the excited state (i.e., the number of long-lived emissive states that occur after initial excitation).[48] Emission decays for ZIF-8 and AuNPs@ZIF-8 were likewise fitted to bi-exponentials, with similar trends across the emission spectrum. The fluorescence emission peak

at 450 nm originates from the ESIPT of the HPBI molecules, as shown previously.[41] This indicates that the structure of HPBI molecules is not fully rigid in the mixture and therefore the non-radiative decay is not fully suppressed.

Table 1. Lifetimes of HPBI, ZIF-8, AuNPs@ZIF-8 and HPBI + ZIF-8/AuNPs@ZIF-8.

	τ_1 (ns), A_1	τ_2 (ns), A_2
ZIF-8	0.87, 87	2.09, 13
AuNPs@ZIF-8-1	0.87, 84	1.96, 16
AuNPs@ZIF-8-2	0.95, 98	2.46, 2
Pure HPBI	0.83, 3	3.79, 97
HPBI + ZIF-8	1.94	
HPBI + AuNPs@ZIF-8-1	1.79	
HPBI + AuNPs@ZIF-8-2	1.94	

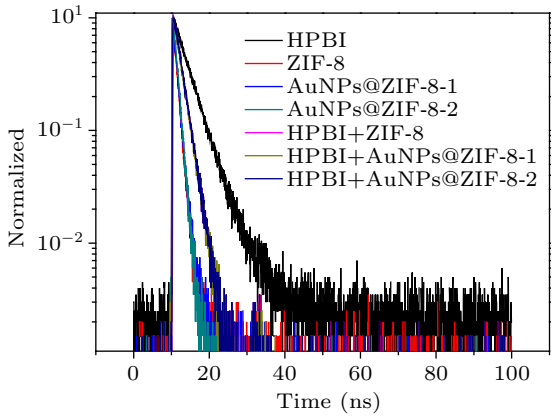


Fig. 5. Dynamics of PL decay of HPBI, ZIF-8, AuNPs@ZIF-8, and HPBI + ZIF-8/AuNPs@ZIF-8.

Refinement of the crystal structure using the superposition of van der Waals atomic radii yielded the aperture and pore size for ZIF-8 (3.4 Å and 11.6 Å, respectively). The structure of ZIF-8, on the other hand, is not set to any particular orientation. Therefore, the pore size of ZIF-8 could not be more restricted to allow only molecules smaller than the pore size to pass, such as the HPBI molecules (3×7 Å) described in this paper. To explain such diffusion, several different mechanisms have been proposed. On the one hand, replacing the coordinately saturated metal center with a dissociative linker could result in a short-lived ligand vacancy, allowing molecules to diffuse into the framework.[49] On the other hand, lattice dynamics in the ZIF-8 framework structure, including collective vibrations or flexibility of MOFs, may lead to processes such as geometrical distortion, shear deformation, or gate opening.[50,51] Thus, gating and kinetic trapping processes are unique to flexible MOFs that allow HPBI molecules to diffuse through the ZIF-8 shell.[16] Though AuNPs are located at the center of ZIF-8 and one side of the HPBI molecule is nearly twice the ZIF-8 pore diameter, the above illustrates that the framework of ZIF-8 crystal is flexible to a certain extent, and that the HPBI molecule still has a greater chance of entering the interior of ZIF-8, due to the local surface of the AuNPs wrapped inside ZIF-8 iso-excited element characteristics of the molecule to produce further enhancement effects on the fluorescence.

The metallic nanodimer (a pair of neighboring nanoparticles) appears to provide a stronger local field surrounding its gap than a single metallic nanoparticle, with the excited emitters having greater quantum yields due to incident light irradiation.[29] As a result, more AuNPs aggregated in HPBI + AuNPs@ZIF-8-2 with gaps which provided a stronger local field. Theoretical calculations of similar metal nanoparticles@MOFs composites in existing research results have demonstrated that the fluorescence enhancement of fluorescent molecules increases as the gap between two metal nanoparticles decreases in a sandwich structure composed of nanoparticles and molecules.[52]

We introduced R6G molecules as a comparison with HPBI. Similar to HPBI, we also deposited R6G powder onto the surface of Au(111) by thermal evaporation and obtained single molecule R6G samples for morphological characterization of the STM topograph in Fig. 6(a). As shown in the STM image, the size of the R6G is around 3 nm, which is too large to pass through the ZIF-8 shell. Using the fluorescence intensity of R6G molecules with different concentrations shown in Fig. 6(b), we found that the peak position of the fluorescence spectrum gradually red-shifted with increasing molecular concentration. The emission peak indicates that the R6G molecules are isolated from each other and fully solvated, hence the emission band around 560 nm.[53]

The fluorescence intensity enhancement of R6G + AuNPs@ZIF-8 and R6G + ZIF-8 at different concentrations is shown in Figs. 6(c)–6(e). From Figs. 6(c) and 6(d), we can see that the highest ΔI of R6G + AuNPs@ZIF-8-1 and R6G + AuNPs@ZIF-8-2 were 2.0 and 2.4, while the highest fold of fluorescence signal enhancement of R6G + ZIF-8 was 1.7. The trend of R6G + AuNPs@ZIF-8-2 was consistent with the HPBI molecules. However, it was found that the fluorescence intensity after 24 h mixing was weakened compared with that after 12 h, and the weakening was more obvious for R6G + AuNPs@ZIF-8-2 (Fig. 6(d)), decreasing to 1.9 corresponding to 0.01 mM. The fluorescence emission efficiency decreased after 24 h of R6G + AuNPs@ZIF-8-2 due to the gold particles, while the ΔI tendencies of R6G + ZIF-8 and R6G + AuNPs@ZIF-8-1 were closer. As a result, in a complicated environment, porous materials with desirable channel widths can be used to size-selectively detect the analytes of interest. For the comparison of energy dispersive x-ray spectroscopy (EDS) results (Fig. 6(f)), after mixing R6G and ZIF-8, the oxygen element of the mixed solution in elemental mapping resembled the results of ZIF-8 alone, and there was no obvious ZIF-8 profile. This means that R6G cannot pass through or adsorb at the aperture of the ZIF-8 (Fig. 6(e)).

As the size of the molecules differed, the fluorescence spectra changed differently, which facilitated the analyte identification.

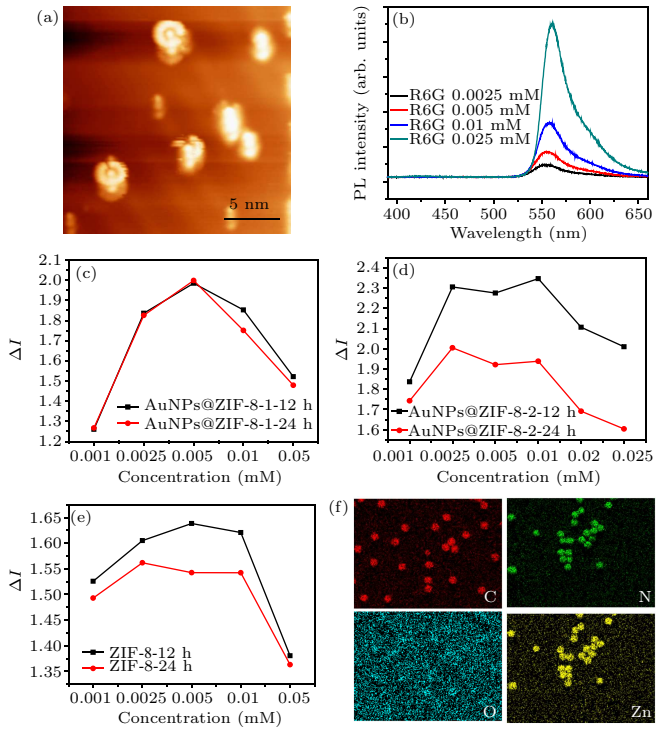


Fig. 6. (a) Typical STM image of R6G on Au(111) (20 nm × 20 nm, −2.5 V, 10 pA). (b) Fluorescence spectra of R6G with different concentrations under excitation at 375 nm. ΔI denotes the enhanced fluorescence intensity of R6G with different concentrations after adding AuNPs@ZIF-8-1 (c), AuNPs@ZIF-8-2 (d) and ZIF-8 (e). (f) Elemental mapping of R6G + ZIF-8.

This phenomenon can be used to improve the accuracy of molecular detection based on pore size matching. Since ZIF-8 has high porosity, it provides space to accommodate guest molecules, increasing the possibility of guest–host interactions and helping to improve the sensitivity of detecting HPBI molecules. The length of one side of the HPBI molecule is nearly twice the pore diameter of ZIF-8, but in this case, because the framework of the ZIF-8 crystal is flexible to a certain extent, the HPBI molecule still has a greater probability of entering the interior of ZIF-8, due to the local surface of the AuNPs wrapped inside the ZIF-8 iso-excited element characteristic of the molecule to produce further enhancement effects on the fluorescence.

To further investigate the role ZIF-8 plays in composites, we defined the composite system with HPBI added during the synthesis as HPBI@ZIF-8, and the composite system with HPBI added after the synthesis as HPBI on ZIF-8. We expected that the addition of HPBI before synthesis would provide the possibility for HPBI to be wrapped in ZIF-8. Figures 7(a) and 7(b) show the corresponding EDS elemental mapping of HPBI on ZIF-8 and HPBI@ZIF-8, and for the sample HPBI@ZIF-8, the distribution of oxygen elements is more obvious than for HPBI on ZIF-8. Both samples were washed three times and the EDS results for HPBI@ZIF-8 illustrate that the HPBI may have been wrapped in ZIF-8, which is not easy to remove.

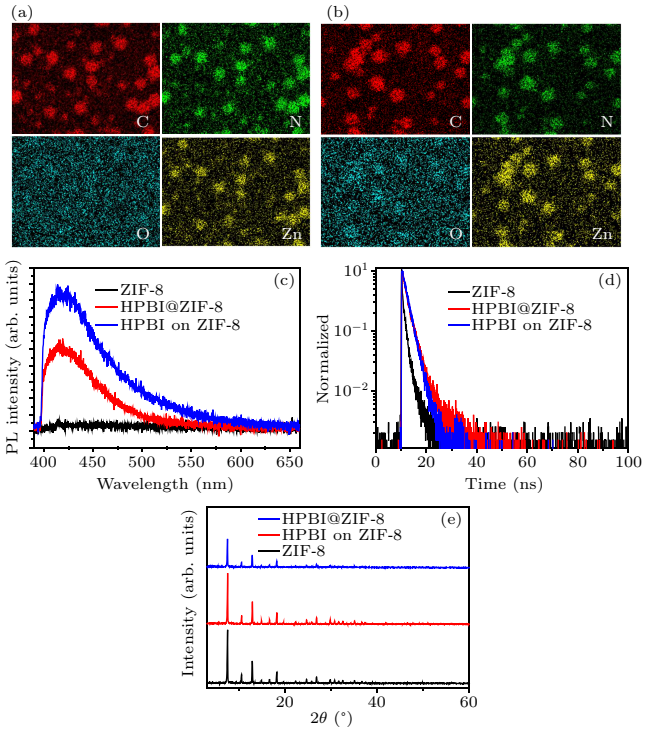


Fig. 7. Elemental mapping of HPBI on ZIF-8 (a) and HPBI@ZIF-8 (b). (c) Fluorescence spectra of ZIF-8, HPBI@ZIF-8 and HPBI on ZIF-8. (d) Dynamics of PL decay of ZIF-8, HPBI@ZIF-8 and HPBI on ZIF-8. (e) X-ray powder diffraction pattern of synthesized HPBI@ZIF-8, HPBI on ZIF-8 and ZIF-8.

The fluorescence spectra of HPBI on ZIF-8 and HPBI@ZIF-8 are consistent, and the sample HPBI on ZIF-8 has a stronger fluorescence intensity than that of HPBI@ZIF-8 (Fig. 7(c)). At this point we estimate that the role of the framework structure of ZIF-8 is in restricting the structure of HPBI molecules within the ESIPT state in both samples. In other words, the enhancement of fluorescence emission intensity at this time is largely derived from the enhancement of the rigid structure of HPBI molecules. When comparing the two different structures, the fluorescence spectra of both the wrapping of HPBI molecules by ZIF-8 and the adsorption of HPBI by the pore of ZIF-8 are close to each other. When comparing the fluorescence lifetimes of HPBI@ZIF-8 and HPBI on ZIF-8,[41] the fluorescence lifetime of HPBI@ZIF-8 is somewhat longer, showing that HPBI on ZIF-8 has a less rigid structure than HPBI@ZIF-8, and hence nonradiative decay pathways are not completely restricted (Fig. 7(d)). The crystallinity of HPBI@ZIF-8 and HPBI on ZIF-8 was demonstrated by the x-ray powder diffraction in Fig. 7(e), which was compared with the ZIF-8 pattern showing no changes in crystallinity.

To further investigate the role of ZIF-8 nanoparticles in modulating the fluorescence of HPBI molecules and the role played by AuNPs in AuNPs@ZIF-8 composite structures, we synthesized HPBI on AuNPs@ZIF-8 and

HPBI@AuNPs@ZIF-8 on the basis of the strategies of HPBI on ZIF-8 and HPBI@ZIF-8. Comparing the TEM of HPBI on AuNPs@ZIF-8 and HPBI@AuNPs@ZIF-8 (Figs. 8(c) and 8(d)), the polyhedral shape of HPBI on AuNPs@ZIF-8 and HPBI@AuNPs@ZIF-8 showed no obvious changes, which is consistent with the results of previous studies. Moreover, the distribution of gold particles distributed in ZIF-8 (Fig. 8(c)) is more dispersed as shown in Fig. 8(d). Combined with this, during the synthesis, we used 1-MI as a linkage bond to form a competitive relationship with Hmim, which in turn regulated the distribution of AuNPs inside ZIF-8. The HPBI molecules also have imidazole rings, which play the same role as their competitors, leading to a more dispersed distribution of gold particles inside ZIF-8 to a certain extent.[11,21] For the emission results, the fluorescence intensity was 2.5 times stronger for HPBI on AuNPs@ZIF-8 than for HPBI@AuNPs@ZIF-8, and the peak position of HPBI@AuNPs@ZIF-8 was redshifted by 15 nm compared with that of HPBI on AuNPs@ZIF-8 (Fig. 8(e)).

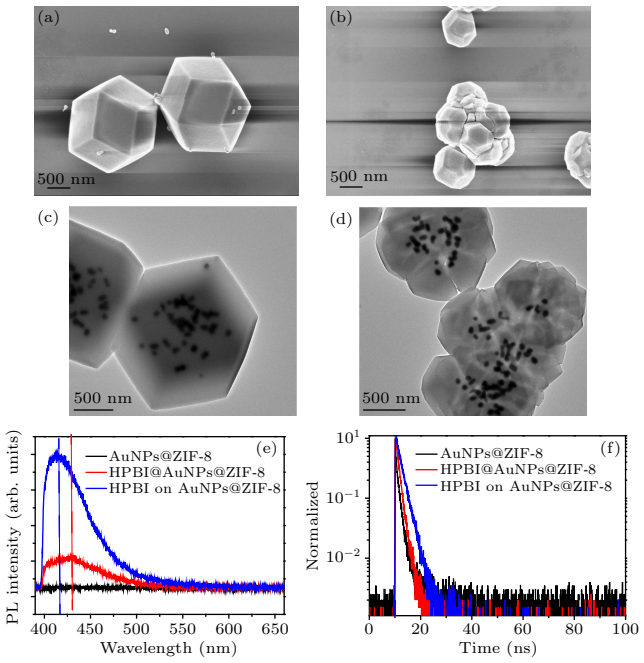


Fig. 8. (a) SEM image of HPBI@AuNPs@ZIF-8. (b) SEM image of HPBI on AuNPs@ZIF-8. (c) TEM image of HPBI@AuNPs@ZIF-8. (d) TEM image of HPBI on AuNPs@ZIF-8. (e) Fluorescence spectra of AuNPs@ ZIF-8, HPBI@AuNPs@ZIF-8 and HPBI on AuNPs@ZIF-8. (f) Dynamics of PL decay of ZIF-8, HPBI@ AuNPs@ ZIF-8 and HPBI on AuNPs@ZIF-8.

When we injected the HPBI molecules and AuNPs into the precursor solution before ZIF-8 formed, the fluorescence intensity was significantly weakened and the fluorescence peak position was red-shifted compared with HPBI on AuNPs@ZIF-8. The results indicated that there was direct contact between the HPBI molecules and AuNPs in ZIF-8, with direct ET occurring resulting in fluorescence quenching. The results for fluorescence decay are also shown in Fig. 8(f). The lifetime of HPBI@AuNPs@ZIF-8 is much shorter than that of HPBI on AuNPs@ZIF-8. Two factors become crucial in multiexponential decay: the individual lives of each component (τ_i) and their fractional contributions (A_i). The total fluorescence lifetime is then computed using the formula $\bar{\tau} = A_1\tau_1 + A_2\tau_2 + \cdots$. HPBI on AuNPs@ZIF-8 and HPBI@AuNPs@ZIF-8 were both best fitted to bi-exponentials, which resulted in spectra of curvature due to the presence of several decay events with characteristic lifetimes (Table 2).

Table 2. The lifetime of HPBI@ZIF-8, HPBI on ZIF-8, HPBI@AuNPs@ZIF-8 and HPBI on AuNPs@ZIF-8.

	τ_1 (ns), A_1	τ_2 (ns), A_2
HPBI@ZIF-8	1.28, 50	3.37, 50
HPBI on ZIF-8	0.90, 19	2.33, 81
HPBI@AuNPs@ZIF-8	0.92, 73	2.13, 27
HPBI on AuNPs@ZIF-8	0.81, 14	2.30, 86

Comparing the results of fluorescence spectra and lifetimes, we found that when HPBI and AuNPs were wrapped into ZIF-8 at the same time, there was constant direct contact between HPBI molecules and AuNPs, which led to fluorescence quenching of HPBI molecules and was accompanied by red-shifting of fluorescence signals. We can see that ZIF-8 acts as a spacer layer in the composite structure AuNPs@ZIF-8 in addition to acting as a molecular sieve. On the basis of the known enhancement of the fluorescence signal of the molecule by the composite structure AuNPs@ZIF-8, the molecule can approach AuNPs through the pore size of ZIF-8 and obtain a certain degree of fluorescence enhancement, and on top of that, ZIF-8 also acts as a spacer layer to avoid direct contact between the molecules and AuNPs. ZIF-8 has a better spacer and screening, and has the potential to be used as a good fluorescence probe.

4. Conclusion and perspectives

In conclusion, we performed fluorescence enhancement using core–shell AuNPs@ZIF-8 composites. The fluorescence enhancement ΔI of HPBI by ZIF-8 was around 55.0, and when we introduced the AuNPs@ZIF-8 composites, ΔI increased to 74.8, with the ability to significantly enhance molecular fluorescence. For comparison, we introduced R6G molecules, which are larger in size than the pores of ZIF-8, and the maximum enhancement effect of AuNPs@ZIF-8 was only 2.4-fold.

An effective strategy to encapsulate HPBI within ZIF-8 was also confirmed, indicating that regardless of the late mixing (HPBI on ZIF-8) or pre-input (HPBI@ZIF-8) to achieve consistent adsorption, the performances of both the fluorescence spectra and lifetimes are similar due to the close size of the HPBI molecule itself to the pore size of ZIF-8. This strategy is also applicable to AuNPs@ZIF-8, allowing the incorporation of AuNPs and small molecules within the MOF matrix.

Based on this synthesis comparison of HPBI on AuNPs@ZIF-8 and HPBI@AuNPs@ZIF-8, it was found that the fluorescence performance of the two structures is completely different, thus showing that ZIF-8 acts as an important spacer layer in this process, and that the spacer layer has a pore size that also has the role of molecular screening.

The AuNPs@ZIF-8 composites were developed to combine the benefits of porosity and molecular sieving behavior, indicated by the MOF matrix with functional behavior characteristics of AuNPs, which led to a considerable enhancement in molecular fluorescence. The preliminary findings establish a scientific foundation for future fluorescence sensing applications.

References

[1] Murray L J, Dinca M and Long J R 2009 *Chem. Soc. Rev.* **38** 1294
[2] Rosi N L, Eckert J, Eddaoudi M, Vodak D T, Kim J, O'Keeffe M and Yaghi O M 2003 *Science* **300** 1127
[3] Li J R, Kuppler R J and Zhou H C 2009 *Chem. Soc. Rev.* **38** 1477
[4] Lee J, Farha O K, Roberts J, Scheidt K A, Nguyen S T and Hupp J T 2009 *Chem. Soc. Rev.* **38** 1450
[5] Ma L, Abney C and Lin W 2009 *Chem. Soc. Rev.* **38** 1248
[6] Allendorf M D, Bauer C A, Bhakta R K and Houk R J 2009 *Chem. Soc. Rev.* **38** 1330
[7] Horcajada P, Chalati T, Serre C, Gillet B, Sebrie C, Baati T, Eubank J F, Heurtaux D, Clayette P, Kreuz C, Chang J S, Hwang Y K, Marsaud V, Bories P N, Cynober L, Gil S, Férey G, Couvreur P and Gref R 2010 *Nat. Mater.* **9** 172
[8] Chae H K, Siberio-Pérez D Y, Kim J, Go Y, Eddaoudi M, Matzger A J, O'Keeffe M and Yaghi O M 2004 *Nature* **427** 523
[9] Bureekaew S, Horike S, Higuchi M, Mizuno M, Kawamura T, Tanaka D, Yanai N and Kitagawa S 2009 *Nat. Mater.* **8** 831
[10] Xiang Z, Hu Z, Cao D, Yang W, Lu J, Han B and Wang W 2011 *Angew. Chem. Int. Ed.* **50** 491
[11] Lu G, Li S, Guo Z, Farha O K, Hauser B G, Qi X, Wang Y, Wang X, Han S, Liu X, DuChene J S, Zhang H, Zhang Q, X Chen, Ma J, Loo S C, Wei W D, Yang Y, Hupp J T and Huo F 2012 *Nat. Chem.* **4** 310
[12] Meilikhov M, Yusenko K, Esken D, Turner S, Van Tendeloo G and Fischer R A 2010 *Eur. J. Inorg. Chem.* **2010** 3701
[13] Liu X Y, F Zhang, Goh T W, Li Y, Shao Y C, Luo L, Huang W, Long Y T, Chou L Y and Tsung C K 2018 *Angew. Chem. Int. Ed. Engl.* **57** 2110
[14] Fang L, Wang W, Liu Y, Xie Z and Chen L 2017 *Dalton Trans.* **46** 8933
[15] Ou J, Zhou Z, Chen Z and Tan H 2019 *Int. J. Mol. Sci.* **20** 4346
[16] Zheng G, de Marchi S, Lopez-Puente V, Sentosun K, Polavarapu L, Perez-Juste I, Hill E H, Bals S, Liz-Marzan L M, Pastoriza-Santos I and Perez-Juste J 2016 *Small* **12** 3935
[17] Kreno L E, Greeneltch N G, Farha O K, Hupp J T and Van Duyne R P 2014 *Analyst* **139** 4073
[18] Park S K, Ni Z, Côté A P, Choi J Y, Huang R, Uribe-Romo F J, Chae H K, O'Keeffe M and Yaghi O M 2006 *Proc. Natl. Acad. Sci. USA* **103** 10186
[19] Liu S, Xiang Z, Hu Z, Zheng X and Cao D 2011 *J. Mater. Chem.* **21** 6649
[20] Ye J W, Zhou H L, Liu S Y, Cheng X N, Lin R B, Qj X L, Zhang J P and X M Chen 2015 *Chem. Mater.* **27** 8255
[21] Zhang W, Zhang Y Y, Bian Y J, Chen M D, Zhang X L, Jin Q Y and Hu B W 2021 *Chin. J. Inorg. Chem.* **37** 2059
[22] Li Z and Zhang Y 2006 *Angew. Chem. Int. Ed.* **45** 7732
[23] Sun Y and Xia Y 2002 *Science* **298** 2176
[24] Vo-Dinh T, Fales A M, Griffin G D, Khoury C G, Liu Y, Ngo H, Norton S J, Register J K, Wang H N and Yuan H 2013 *Nanoscale* **5** 10127
[25] Chen W, Hu H T, Jiang W, Xu Y H, Zhang S P and Xu H X 2018 *Chin. Phys. B* **27** 107403
[26] Thomas M, Greffet J J, Carminati R and Arias-Gonzalez J R 2004 *Appl. Phys. Lett.* **85** 3863
[27] Carminati R, Greffet J J, Henkel C and Vigoureux J M 2006 *Opt. Commun.* **261** 368
[28] Li T, Yu L, Lu Z-X, Song G and Zhang K 2011 *Chin. Phys. B* **20** 087805
[29] Liaw J W, Chen C S and Chen J H 2010 *J. Quant. Spectrosc. Radiat. Transfer* **111** 454
[30] Colas des Francs G, Bouhelier A, Finot E, Weeber J C, Dereux A, Girard C and Dujardin E 2008 *Opt. Express* **16** 17654
[31] Yin T T, Jiang L Y, Shen Z X 2018 *Chin. Phys. B* **27** 097803
[32] Ding Q, Wang J, Chen X, Liu H, Li Q, Wang Y and Yang S 2020 *Nano Lett.* **20** 7304
[33] Tam F, Goodrich G P, Johnson B R and Halas N J 2007 *Nano Lett.* **7** 496
[34] Hermes S, Schroter M K, R Schmid, Khodeir L, Muhler M, Tissler A, Fischer R W and Fischer R A 2005 *Angew. Chem. Int. Ed. Engl.* **44** 6237
[35] Jiang H L, Liu B, Akita T, M Haruta, Sakurai H and Xu Q 2009 *J. Am. Chem. Soc.* **131** 11302
[36] Esken D, Turner S, Lebedev O I, Van Tendeloo G and Fischer R A 2010 *Chem. Mater.* **22** 6393
[37] Jiang H L and Xu Q 2011 *Chem. Commun.* **47** 3351
[38] Falcaro P, Hill A J, Nairn K M, Jasieniak J, Mardel J I, Bastow T J, Mayo S C, Gimona M, Gomez D, Whitfield H J, Ricco R, Patelli A, Marmiroli B, Amenitsch H, Colson T, Villanova L and Buso D 2011 *Nat. Commun.* **2** 237
[39] Sugikawa K, Furukawa Y and Sada K 2011 *Chem. Mater.* **23** 3132
[40] Zhang Y, Zhang W, Bian Y, Liu Y, Zhang X, Chen M, Hu B and Jin Q 2022 *RSC Adv.* **12** 9342
[41] Konoshima H, Nagao S, Kiyota I, Amimoto K, Yamamoto N, Sekine M, Nakata M, Furukawa K and Sekiya H 2012 *Phys. Chem. Chem. Phys.* **14** 16448
[42] de Vivie-Riedle R, De Waele V, Kurtz L and Riedle E 2003 *J. Phys. Chem. A* **107** 10591
[43] Zheng J J, Zhang G L, Guo Y X, Li X P and Chen W J 2007 *Chin. Phys.* **16** 1047
[44] Mei J, Leung N L, R T Kwok, Lam J W and Tang B Z 2015 *Chem. Rev.* **115** 11718
[45] Zhong Y, Chen C, Liu S, Lu C, Liu D, Pan Y, Sakiyama H, Muddassir M and Liu J 2021 *Dalton Trans.* **50** 18016
[46] Wu C S, Xiong Z H, Li C and Zhang J M 2015 *RSC Adv.* **5** 82127
[47] Bauer C A, Timofeeva T V, Settersten T B, Patterson B D, Liu V H, Simmons B A and Allendorf M D 2007 *J. Am. Chem. Soc.* **129** 7136
[48] Urbina-Villalba G and García-Sucre M 2001 *Colloids Surf. A* **190** 111
[49] Morabito J V, Chou L Y, Li Z, Manna C M, Petroff C A, Kyada R J, Palomba J M, Byers J A and Tsung C K 2014 *J. Am. Chem. Soc.* **136** 12540
[50] Fletcher A J, Thomas K M and Rosseinsky M J 2005 *J. Solid State Chem.* **178** 2491
[51] Ryder M R, Civalleri B, Bennett T D, Henke S, Rudic S, Cinque G, Fernandez-Alonso F and Tan J C 2014 *Phys. Rev. Lett.* **113** 215502
[52] A Bek, Jansen R, Ringler M, Mayilo S, Klar T A and Feldmann J 2008 *Nano Lett.* **8** 485
[53] Zehentbauer F M, Moretto C, Stephen R, Thevar T, Gilchrist J R, Pokrajac D, Richard K L and Kiefer J 2014 *Spectrochim. Acta A Mol. Biomol. Spectrosc.* **121** 147